

## SPECIFIC FEATURES OF EXCITATION OF PERIODIC WAVEGUIDE SURFACE FIELD AT THE BOUNDARY CUTOFF FREQUENCY

V. I. Kanavets, A. S. Nifanov, and A. I. Slepko

Methods of the linear multimode theory and nonlinear nonstationary theory were employed to study the specific features of self-consistent interaction between the surface field of a superdimensional periodic waveguide and a relativistic heavy-current tubular electron beam. The longitudinal and transverse structures of the electromagnetic field, the efficiency, and the generation spectrum were found.

### INTRODUCTION

The energy exchange between the electron beam and the electromagnetic field improves when there is beam field synchronism in the vicinity of the boundary cutoff frequency. In this case the amplification increases, and the start currents corresponding to the beginning of the generation attain minimum values. This feature of the processes is used for the electronic selection of modes in relativistic generators on superdimensional waveguides [1-4]. However, the effect of the beam on the selection mechanism is not yet thoroughly studied. In particular, this refers to the effect of the beam on the "hot" shift of the boundary cutoff [2] and on the conditions of synchronism. The electron medium displaces the flow-field synchronism point toward lower values of the longitudinal wavenumber  $k_z$  (toward the traveling-wave tube regime), and often determines the generation frequency and the structure of the amplified field [5].

The self-consistent mechanism of the resonant flow-field interaction of a periodic waveguide in the vicinity of the boundary cutoff frequency possesses important peculiarities in the linear and nonlinear regimes [6, 7]. In some cases this mechanism leads to the formation of specific surface and electron modes in both the amplifiers and the generators. The present paper is devoted to a theoretical analysis of specific features of excitation of surface fields in a periodic waveguide with the aid of a relativistic electron flow in the vicinity of the boundary cutoff frequency of the lower axisymmetric mode.

### 1. METHODS OF THE LINEAR AND NONLINEAR THEORIES

The consideration of the fields in a periodic waveguide in the linear approximation is based on the multimode network method [8]. A section of a superdimensional periodic waveguide is divided into several auxiliary regions by planes perpendicular to the axis of the system (Fig. 1 a). In each region the curling field is expanded with respect to the complete system of orthogonal functions determining the modes of the corresponding smooth waveguide. Transfer matrices are introduced for the amplitudes of the electromagnetic field modes, which are excited between the adjacent cross sections, and of the electron flow waves. The transfer matrices are constructed for the fields and electron waves in separated regions within the limits of one period of the structure.

The transfer matrix  $G$  for the fields and the beam waves on a separate period of the system is used to determine the dispersion characteristics and the structure of natural waves of a periodic waveguide with a

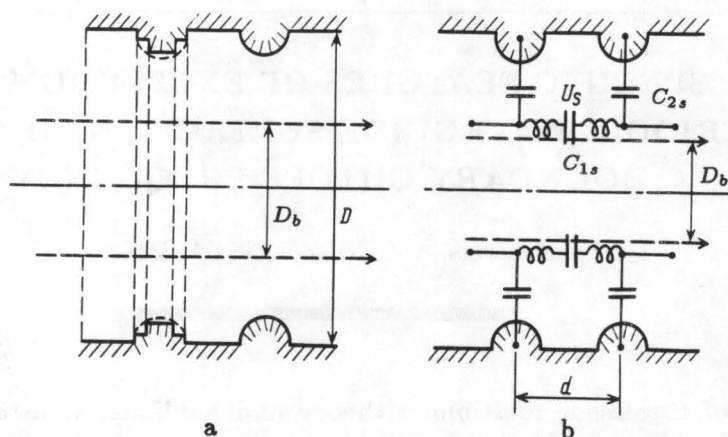


Fig. 1

(a) Schematic diagram of a typical periodic waveguide with an electron beam. (b) The equivalent circuit:  $D$  and  $D_b$  are the waveguide and beam radii, respectively,  $U_s$  is the voltage at the beam-field interaction gap, and  $d$  is the period of the system.

relativistic electron beam [6]. The propagation constants of the coupled system are found from the dispersion relation

$$\det(G - e^{\Gamma} I) = 0,$$

where  $\Gamma = \alpha + i\varphi$ ,  $\alpha$  is the build-up constant,  $\varphi$  is the phase shift on a period, and  $I$  is the unit matrix. The structure of natural waves is found from the solution of a problem on the eigen vectors for the same matrix.

To investigate the physical processes we consider the axisymmetric modes of the equivalent smooth waveguides corresponding to the most efficient beam-field interaction. In the solution process we separate out the eigen waves of a system with a beam that correspond to the field surface modes and to the electron beam modes in the waveguide.

The theoretical analysis of the way the oscillations set up in a Cerenkov generator is carried out within the framework of a nonlinear nonstationary technique. It is based on the assumption that in the Cerenkov generator in question the electrons predominantly interact with the surface wave field. The role of the bulk fields reduces to additional synchronization of the interaction space and the withdrawal of the microwave energy. These features of the beam radiation in a superdimensional periodic waveguide are confirmed by the multimode method data (see Sections 2 and 3). The above assumption makes it possible to resort to an approximate one-mode nonlinear technique based on the description of the surface wave field using a chain of four-terminal networks that is replaced by an equivalent circuit [4].

The equivalent circuit of a section of the device is shown in Fig. 1b. The resultant longitudinal conductivity is of inductive character, which corresponds to the positive dispersion. The parameters of the equivalent circuit for the surface wave are selected by analogy with [5]. The amplitudes of the electric field intensities in the capacitances  $C_{1s}$  and  $C_{2s}$  correspond to the intensities of the longitudinal and transverse electric field components in the surface wave. The effect of the beam is included by introducing an induced current  $I_{is}$  into the equivalent circuit, which, generally, can have both the longitudinal and transverse components.

Within the framework of the chosen model of analysis of nonstationary processes, the assumption is made that the processes vary slowly in time and that the second derivatives of all the variables are negligibly small as compared to the first derivatives. In particular, a reference frequency  $\omega$  is singled out, which is equal to the frequency of the kinematic beam-field synchronism. The excitation equations and the equations of motion are given in the Supplement.

The resulting system of equations is solved using a non-obvious two-stratum scheme with forestallation. The time derivatives are written in the form

$$U'_s = (\hat{U}_s - U_s)/\tau,$$

where  $U_s$  and  $\widehat{U}_s$  are the voltages in the gap with the subscript  $s$  at the present and future time instants (they are normalized to the accelerating voltage  $V_0$ ) and  $\tau = \omega t$  is the normalized time. The excitation equation is written in discrete form as

$$\begin{aligned} & \widehat{U}_{s+1}(A_s - \tau E_s) + \widehat{U}_s(B_s - \tau F_s) + \widehat{U}_{s-1}(C_s - \tau H_s) \\ & = U_{s+1}A_s + U_sB_s + U_{s-1}C_s + I_{is+1}\tau H_s + I_{is}\tau P_s + I_{is-1}\tau Q_s + I'_{is}\tau R_s, \end{aligned}$$

where the coefficients  $A_s, B_s, C_s, H_s, P_s, Q_s,$  and  $R_s$  are determined in the Supplement.

The system of excitation equations is solved at each step by means of the factorization method. After that the equations of motion are solved and the induced current in each cell is found. The resulting data on the fields in the gaps are used to determine the interaction efficiency and the radiation spectrum.

## 2. FIELDS AND WAVES IN THE AMPLIFIER AND THE GENERATOR

First of all we consider the results of a numerical analysis of the formation of the surface and the electron modes in relativistic amplifiers of large diameter ( $D > \lambda$ ) for currents  $I_0 \simeq 1$  kA and voltages  $V_0 \simeq 0.3$ –1 MV. Most frequently these modes are increasing eigen waves of the system (a beam in the waveguide), and they characterize the signal amplification.

The structure of the fields of eigen waves is determined in the form of superposition of the modes of a reference smooth waveguide and the space charge waves. This, in turn, makes it possible to determine the sign of the power carried away by the electromagnetic field of an individual wave. We assume that each of the four combinations of the imaginary part  $\text{Im}(k_z d/\pi)$  of the propagation constant and of the power  $P_v$  of the curling field corresponds to an eigen wave of the periodic waveguide. This makes it possible to separate the regimes of amplification and attenuation for both the forward and the backward waves.

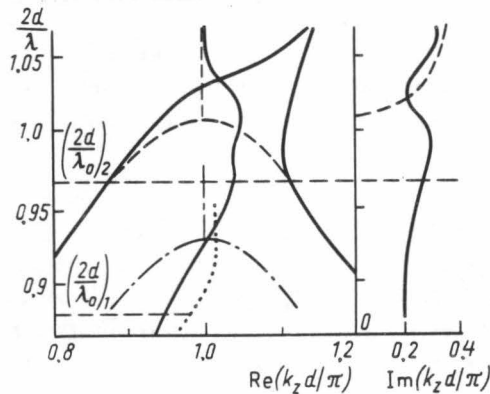


Fig. 2

Dispersion characteristics of a periodic waveguide in the regime of excitation of a surface (subscript "1") and a bulk (subscript "2") wave. The dashed lines: bulk wave without a beam; the dash-and-dot line: surface wave without a beam; the solid lines: wave in a weakly corrugated system with a beam; the dotted line: complex solution for a system with a surface wave and a beam.

When there is synchronism, in a frequency range near the  $\pi$  form, we note specific complex solutions to the dispersion equation on the obtained dispersion characteristics (Fig. 2). In the range of upper frequencies, two (increasing and decreasing) eigen waves of the "hot" superdimensional periodic waveguide correspond to these solutions. These waves have the same transverse structures, and the sum of the powers of the electromagnetic curling field and the kinetic power of the electron beam is equal to zero for them. The behavior of the dispersion curves is similar to that of the curves obtained by the method of equivalent circuits [5].

From the standpoint of the theory of coupled waves, for a definite range of voltages in the system there arises a beam-excited four-wave interaction of the fast and the slow space charge waves with the forward and backward waveguide waves (see Fig. 2). On the line corresponding to the complex root the region of reactive attenuation turns smoothly into the condition of active coupling of the slow space charge wave with the forward spatial harmonic of the mode  $E_{01}$ , after which it goes into the region of convective instability (corresponding to the interaction between the fast and the slow space charge waves owing to the effect of the walls).

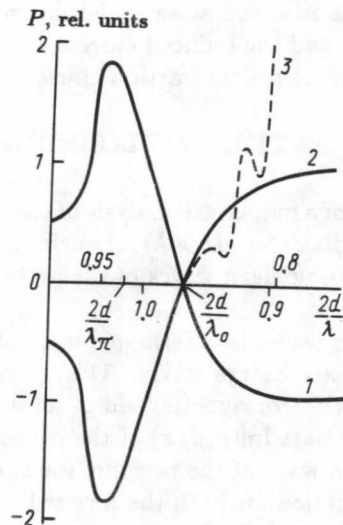


Fig. 3

Power flow components for the increasing wave in an infinite waveguide: (1) kinetic power in the beam; (2) curling field power; (3) curling field power flow in a finite-length system. The upper and lower scales refer to the values of  $2d/\lambda$  corresponding to the surface and bulk waves, respectively.

The frequency dependence of the power of the beam and curling field waves, which corresponds to the complex solution to the dispersion equation, is demonstrated in Fig. 3. The Umov-Pointing vector of the curling field changes sign at  $2d/\lambda = 0.97$ . This value of  $2d/\lambda$  can be called the "hot" boundary cutoff, and in the range of large frequencies a reactive attenuation is observed for waves with complex propagation constants. For smaller values of  $2d/\lambda$  we have  $P_v > 0$  for the electromagnetic field power flow,  $\text{Im}(k_z d/\pi) > 0$ , and amplification of the input signal is observed along the system.

The conclusion that amplification takes place at precisely these frequencies is also confirmed by the calculations conducted for a periodic waveguide section having 30 periods with consideration for reflected waves at the input and output. The field of the section was excited by the mode  $E_{01}$  of the smooth waveguide. The dashed line in Fig. 3 represents the field power at the output of the system as a function of frequency. For  $2d/\lambda < 0.97$  the output power is insignificant, and it increases with decreasing frequency. Owing to the mismatching of the input and output loads, the frequency dependence has a clearly resonance character.

Consider the field structure of eigen waves of the periodic waveguide that correspond to the complex root of the dispersion equation (Fig. 4 a). In the region of reactive attenuation ( $2d/\lambda = 1.03$ ), when there is no electron beam, the structure of eigen waves is similar to that of the bulk field of the mode  $E_{01}$  for the smooth waveguide. The beam effect results in the formation of a weak maximum of the longitudinal field  $E_z$  in the vicinity of the beam.

As one moves along the line of the complex root toward lower frequencies, the bulk field at the center of the waveguide decreases and the field in the region of the beam increases ( $2d/\lambda = 0.974$ ; Fig. 4 a). In the structure of the electron mode field there appear a maximum and minimum. The depth of the minimum increases with further decrease of frequency. In the region of convective instability ( $2d/\lambda < 0.94$ ; Fig. 4 a)

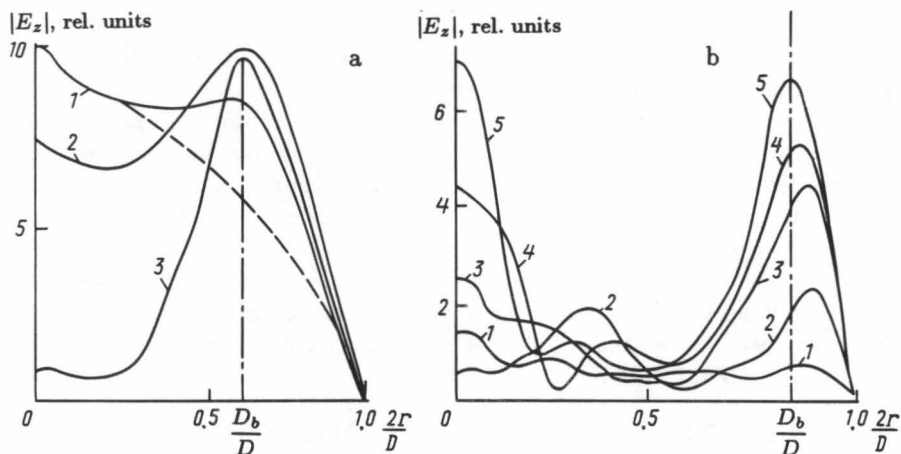


Fig. 4

Radial variation of the longitudinal component of the electric field: (a) for an eigen wave of the periodic waveguide without beam (dashed curve) and for an increasing eigen wave (solid curves),  $2d/\lambda = 1.03$  (1),  $0.974$  (2), and  $0.94$  (3); (b) in a finite-length system,  $z/L = 0.1$  (1),  $0.3$  (2),  $0.5$  (3),  $0.7$  (4), and  $1$  (5). The vertical dash-and-dot line shows the position of the electron beam.

the bulk field tends to zero. In this case the electron wave structure generally corresponds to the curling field, with a maximum in the vicinity of the beam, which is entrained by the beam.

For the given magnitudes of currents and voltages and at the frequencies under consideration, the electron beam substantially perturbs the curling fields of the periodic waveguide. The field structure is determined by the beam, which corresponds to the formation of an electron mode in the amplifier section, and, from the standpoint of the actual constructions, this regime corresponds to the amplification in the intermediate sections [6].

### 3. EXCITATION OF THE SURFACE FIELD

When studying the beam-field interaction processes in the system with inclusion of input and output loads, we selected a 10-period section of the periodic waveguide. With this length of the section, in a system without a beam mainly surface waves are excited because in this case there are no resonance conditions needed for the excitation of bulk waves. The calculations by an iterative technique [7, 8] showed that for a current of 10 kA the self-excitation arises when the section length has 12 or 13 periods. Thus, with the length of 10 periods one deals with the amplification conditions.

In analyzing the beam-field interaction in the sections of the device under study we apply the ideal matching approximation under which the wave of each mode of the smooth waveguide in the absence of the beam is not reflected and is not transformed into other modes at the ends of the system. This situation corresponds to the experimental conditions when special matching horns are used [9] and one can assume that the output and input of the periodic waveguide section are joined to semi-infinite smooth waveguides. We shall also assume that the amplitudes of forward waves are set at the input of the one-section system, there are no incident waves at the output, and we have to determine the radiation fields from the section of the periodic waveguide.

Let us study the excitation of curling fields in the first section of the Cerenkov source. The field in the system was excited by the mode  $E_{01}$  of the smooth waveguide. Fig. 4b illustrates the distribution of the longitudinal component  $E_z$  of the curling field in the Cerenkov section in question at the exit of the first (curve 1), third (curve 2), fifth (curve 3), seventh (curve 4), and tenth (curve 5) periods at the wavelength  $2d/\lambda = 0.82$ . The field inside the system is close to the surface field. The synchronism of the electron flow and the field of the surface wave results in a substantial increase of the surface component of the field along

the system. In the vicinity of the section exit a maximum of the bulk field is formed at the waveguide axis, which is mainly related to the surface wave field scattering by periodic inhomogeneities of the finite-length waveguide. Note that with decreasing beam current the maximum value of the field at the waveguide axis decreases, and the role of the surface field increases. A similar result is obtained under the excitation of the output section by an initially current-modulated beam.

Thus, for certain parameters, surface waves are primarily excited not only in an infinite-length system but also in a finite-length system. This makes it possible to investigate nonlinear stationary processes in a system using a superdimensional waveguide in the one-mode approximation and employ, for example, the method of equivalent circuits. The parameters of an equivalent circuit can be found in preliminary calculations using the linear network technique.

We note that the appearance of a wide-band convective instability in the electron beam is related to the strong effect of walls on the processes in the beam. This circumstance enables one, when describing nonlinear nonstationary processes, to neglect forces of the space charge and to confine oneself to the kinematic approximation.

#### 4. NONSTATIONARY PROCESSES IN THE GENERATOR

To consider the efficiency of the Cerenkov radiation at frequencies near the  $\pi$ -form boundary cutoff, the case of ideal "cold" matching was chosen when loads that are exactly equal to the wave impedance of an infinite system are set at the ends of the system in question. The investigation of the generation efficiency was carried out for different values of  $k_{z0}d$ , which is the electron transit angle for one period of the system and is found from the condition of kinematic synchronism of the beam and the field.

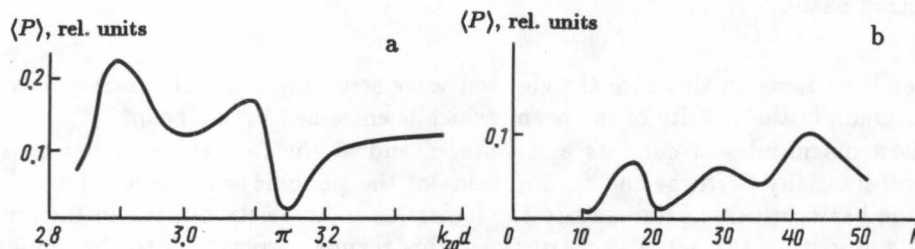


Fig. 5

Dependence of the mean generation power on the parameter  $k_{z0}d$  (a) and on the number  $N$  of periods of the waveguide section (b).

The dependence of the mean generation power  $\langle P \rangle$  normalized to the beam power on the value of  $k_{z0}d$  for a one-section generator is demonstrated in Fig. 5 a. At the  $\pi$ -form frequency ( $k_{z0}d = \pi$ ) the radiation intensity attains minimum values. A small increase in the transit angle  $k_{z0}d$  results in an increase of the output power. In all cases, interaction mechanisms of the backward-wave-tube and traveling-wave-tube types are simultaneously present in the system. Interaction between the beam and the backward harmonic determines the magnitude of the internal feedback and the self-excitation conditions for the section (the starting length and current), and the interaction with the forward wave produces an additional amplification. In particular, an increase in the accelerating voltage related to an increase of the contribution from the traveling-wave-tube mechanism results in an increase of the output power. The data of a numerical analysis confirm this assumption, i. e., the smaller the transit angle, the higher the radiation efficiency (see Fig. 5).

Under all operation conditions corresponding to Fig. 5, the generation frequency does not coincide with the frequency of the beam-field kinematic synchronism and undergoes a 1-2% shift toward lower frequencies (Fig. 6). This fact is in agreement with the conclusions drawn from the linear analysis (see Sections 2 and 3) that in the beam-field interaction at frequencies in the neighborhood of the  $\pi$ -form oscillations there occurs an electron shift of the boundary of the transmission band toward lower frequencies, and the generation arises first of all at "hot" boundary cutoff frequencies.

An analysis of the generation in systems of different lengths showed that the generation frequency mainly depends on the waveguide properties of the system, i. e., the generation frequency does not depend

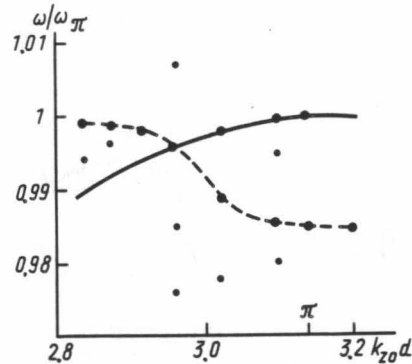


Fig. 6

Normalized values of the kinematic synchronism frequency (solid curve) and of the generation frequency (dashed curve) versus  $k_{z0}d$ . The dots represent the frequencies of additional maxima in the generation spectrum.

very much on the system length. In these conditions the magnitude of the positive feedback is primarily determined by the internal coupling, and reflections from the ends of the system that arise upon introduction of an electron beam lead to additional resonances as the length of the system changes and these affect the generation efficiency (Fig. 5b).

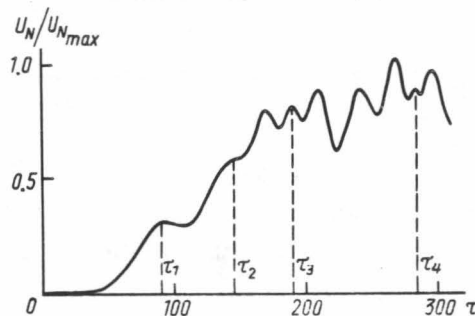


Fig. 7

Normalized values of the voltage amplitude  $U_N$  at the generator output versus time  $\tau = \omega t$ .

More complex processes of oscillation growth develop in a two-section system. As in the case of a separate section, the beam-field synchronism for the fundamental spatial harmonic is observed in the neighborhood of the  $\pi$ -form frequency, and the presence of first maxima in the dependence of the field amplitude at the output of the system on time can be associated to the characteristic times of the development of the processes in the sections. These relationships are most pronounced in nonoptimal regimes of operation. In particular, the first and second maxima ( $\tau = \tau_1$  and  $\tau = \tau_2$ ) in Fig. 7 are related to the closure of the feedback circuit arising owing to the reflections in the second section. The maximum corresponding to  $\tau = \tau_3$  (see Fig. 7) is formed as a result of the closure of the feedback circuit in the first section. The characteristic closure time of the feedback circuit for the entire system is equal to  $\tau_4$ . On the  $U_N(\tau)$  curve the maximum at  $\tau = \tau_4$  corresponds to this time.

Upon optimization of the parameters of a two-section generator its efficiency may substantially exceed the maximum efficiency of a one-section generator. Figure 8 demonstrates the process of development of oscillations in a two-section generator with a maximum efficiency exceeding 30%. The generation spectrum is close to a single-frequency spectrum with a small magnitude of the additional components. The resulting

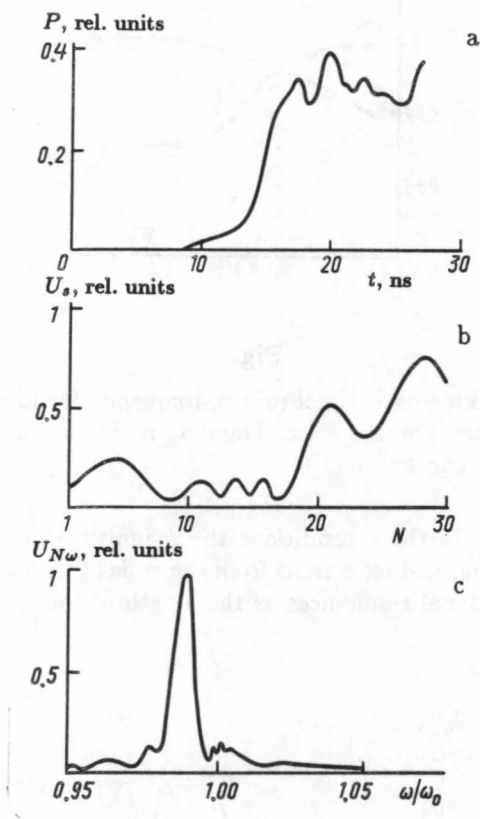


Fig. 8

Typical characteristics of a two-section Cerenkov generator: (a) variation of the generation power in time; (b) voltage distribution along the system; (c) generation spectrum.

optimal field distribution is characterized by the excitation of the fundamental longitudinal mode in the first section and by a traveling-wave-tube type distribution in the second section. In the drift space there appears a field close to that of a standing wave.

## CONCLUSION

The study carried out using the multimode network method has shown that in heavy-current spatially developed Cerenkov sources on periodic waveguides that operate at electron energies below 1 MeV the dominant role is played by the excitation of surface fields. At frequencies of the boundary cutoff the effect of the beam results in a low-frequency shift of the "hot" boundary cutoff (into the transmission band). The nonlinear nonstationary analysis data showed that self-excitation of the system occurs at frequencies lying inside the band boundary, and the radiation power is minimum in the immediate vicinity of the  $\pi$ -form. It is shown that sectioning of the system ensures a higher generation efficiency.

SUPPLEMENT

The excitation equations for an equivalent circuit written with selection of a reference frequency for capacitive gaps have the form

$$\begin{aligned}
 A_s U'_{s+1} + B_s U'_s + C_s U'_{s-1} &= E_s U_{s+1} + F_s U_s + G_s U_{s-1} + H_s I_{is+1} + P_s I_{is} + Q_s I_{is-1} + R_s I'_{is}; \\
 A_s &= \frac{C_{2s+1}}{i\omega L_s^2 C_{2s} C_{1s+1}}; \quad C_s = \frac{C_{2s-1}}{i\omega^2 L_s C_{2s} C_{1s}}; \\
 B_s &= -\frac{C_{2s+1}}{i\omega^2 L_s C_{2s}} \left( \frac{1}{C_{1s+1}} + \frac{1}{C_{1s}} \right) + \frac{\omega^2 L_s C_{2s} - 1}{i\omega^2 L_s C_{2s}} - 2i; \\
 E_s &= -\frac{C_{2s+1}}{C_{1s+1}}; \quad G_s = -\frac{C_{2s-1}}{\omega^2 L_s C_{2s} C_{1s}}; \\
 F_s &= \frac{1}{\omega^2 L_s C_{2s}} \left( \frac{1}{C_{1s+1}} + \frac{1}{C_{1s}} \right) + \frac{1}{i\omega^2 L_s C_{2s}} - 1; \\
 H_s &= -\frac{i}{\omega^3 L_s C_{2s} C_{1s+1}}; \\
 P_s &= \frac{i}{\omega^3 L_s C_{2s}} \left( \frac{1}{C_{1s+1}} + \frac{1}{C_{1s}} \right) - \frac{i}{\omega C_{2s}}; \\
 Q_s &= -\frac{i}{\omega^3 L_s C_{2s} C_{1s}}; \quad R_s = -\frac{2}{\omega C_{2s}},
 \end{aligned}$$

where  $L_s$ ,  $C_{1s}$ , and  $C_{2s}$  are the parameters of the equivalent circuit,  $I_{is}$  is the induced current, and  $s$  is the index of the cell under consideration ( $s = 1, \dots, S$ ).

The equations of beam motion are written for the discrete model of large particles. The assumption of slow variation of the processes in time permits their representation in the phase coordinate system  $\Phi = \Phi(\Phi_0, y)$ :

$$\Phi_m'' = -(1 + \Phi_m')^3 \left[ 1 - \left( \frac{v_0/c}{1 + \Phi_m'} \right)^2 \right]^3 \frac{e/m_0}{\omega v_0} E_{sz},$$

where  $E_{sz} = MU_s/l$ ;  $I_i = (M/mk)\Sigma e^{i\Phi_m}$ ;  $G_0 = I_0/V_0$ ;  $\tau = \omega_0 t$ ;  $M$  is the beam-field interaction coefficient;  $l$  is the equivalent width of the interaction gap;  $\Phi_m$  is the phase of the  $m$ th particle ( $m = 1, \dots, mk$ );  $\Phi_{m_0}$  is the phase of getting into the first gap; and  $y = \beta_e z$  is the normalized current coordinate.

The equations of motion and the excitation equations are supplemented with boundary and initial conditions written for voltages at the interaction gaps. At the system input they have the form

$$A_1 U_2 + B_1 U_1 = E_1 U_2 + F_1 U_1 + H_1 I_{i2} + P_1 I_{i1} + R_1 I'_{i1} + C_{12} i\omega \epsilon_0,$$

where

$$\begin{aligned}
 A_1 &= -C_{22}\omega; \quad B_1 = \omega C_{12} + \omega C_{21} + \omega^2 Z_0 \times 2iC_{12}C_{21} - 3L\omega^3 C_{21}C_{12}; \\
 E_1 &= -iC_{22}\omega; \quad F_1 = -i(\omega C_{12} + C_{21}) + \omega^2 Z_0 C_{12}C_{21} - 3iL\omega^3 C_{21}C_{12}; \\
 H_1 &= -1; \quad P_1 = i\omega C_{12}Z_0 - C_{12}L_1\omega^2 + 1; \quad R_1 = \omega Z_0 C_{12} + 2iL_1\omega^2 C_{12}.
 \end{aligned}$$

At the system output we have

$$C_S U_{S-1} + B_S U_1 = G_S U_{S-1} + F_S U_S + R_S I'_{iS} + H_S I_{iS-1} + P_S I_{iS},$$

where

$$\begin{aligned}
 C_S &= -C_{2S-1}\omega; \quad B_S = \omega C_{1S} + \omega C_{2S} + \omega^2 Z_S \times 2iC_{1S}C_{2S} - 3L_S\omega^3 C_{2S}C_{1S}; \\
 G_S &= iC_{2S-1}\omega; \quad F_S = -i(\omega C_{1S} + C_{2S}) + \omega^2 Z_S C_{1S}C_{2S} + iL_S\omega^3 C_{2S}C_{1S}; \\
 H_S &= -1; \quad P_S = i\omega C_{1S}Z_S - C_{1S}L_S\omega^2 + 1; \quad R_S = \omega Z_S C_{1S} + 2iL_S\omega^2 C_{1S},
 \end{aligned}$$

the initial conditions are written as

$$U_s|_{\tau=0} = U_s^0; \quad \Phi_m|_{s=1} = \frac{2\pi m}{mk}; \quad \Phi_m|_{s=1} = 0.$$

## REFERENCES

1. S. P. Bugaev, V. I. Kanavets, V. I. Koshelev, et al., *Relativistic High-Frequency Electronics* (in Russian), no. 5, p. 78, Gorky, 1988.
2. V. I. Kanavets, Yu. D. Mozgovoï, and A. I. Slepko, *Radiation of Powerful Electron Flows in Resonant Decelerating Systems* (in Russian), Moscow, 1993.
3. S. P. Bugaev, V. I. Kanavets, V. I. Koshelev, and V. A. Cherepenin, *Relativistic Multiwave Microwave Generators* (in Russian), Novosibirsk, 1991.
4. N. A. Garutsa, V. I. Kanavets, and A. I. Slepko, *Vest. Mosk. Univ. Fiz. Astron.*, vol. 27, no. 4, p. 37, 1986.
5. V. I. Kanavets, A. S. Nifanov, and A. I. Slepko, *Vest. Mosk. Univ. Fiz. Astron.*, vol. 31, no. 5, p. 34, 1990.
6. V. I. Kanavets, A. S. Nifanov, and A. I. Slepko, *Vest. Mosk. Univ. Fiz. Astron.*, vol. 31, no. 6, p. 80, 1990.
7. V. I. Kanavets, N. S. Kaeva, and A. I. Slepko, in: *Physics and Applications of Microwaves* (in Russian), Part 1, p. 22, Moscow, 1991.
8. N. A. Garutsa, V. I. Kanavets, and A. I. Slepko, *Radiotekhn. Elektron.*, vol. 33, no. 4, p. 783, 1988.
9. V. I. Kanavets, A. S. Nifanov, and A. I. Slepko, in: *Abstracts of the 10th USSR Seminar on Wave and Oscillation Phenomena in O-Type Electronic Instruments* (in Russian), p. 62, Leningrad, 1990.